A RE-ASSESSMENT OF DUCTILE TEARING RESISTANCE. PART II: ENERGY DISSIPATION RATE AND ASSOCIATED R-CURVES ON NORMALISED AXES.

C.E. Turner †

The many J-R-curves in plastic bending fall into a pattern in terms of the maximum plastic zone size for a given material in relation to the size of test piece. The 'wider-lower' case is analysed by dU_{dis}/Bda as a reducing function of $(\Delta a/b_o)(S/b_o)$, where dU_{dis} is the increment of (external work minus the internal elastic strain energy). This term automatically reduces to the I energy rate model for ductile tearing instability.
A geometry independent rising R-curve is obtained on an abscissa of $\Delta a/b_o$, provided S/b_o is constant. If dU_{dis}/Bda is also normalised by the maximum possible dissipation rate for the material, then geometry independent R-curves emerge for other bending cases. This normalisation of fully plastic R-curves on both axes is seen as an extension of the analysis for contained yield, by Rice *et al* , into uncontained yield.
One set of data, for which J-R-curves would be 'wider-higher', allow the dissipation rate to be split into flat (areal) and slant (volumetric) components, promising a more fundamental understanding of the effects of both width and thickness if data were analysed in this way.

INTRODUCTION

In this part of the paper more detailed data and arguments are presented in support of the general ideas advanced in Part I. It is quite apparent that the data are indicative rather than conclusive. Nevertheless, the writer believes that the plasticity viewpoint as here presented, offers a unified picture of ductile tearing behaviour with fewer inconsistencies than the conventional J-R interpretation.

THE GEOMETRY DEPENDENCE OF J-R CURVES IN UNCONTAINED YIELD

Some examples of different behaviours were shown Fig.4. all pertaining to the deep notch bending and compact tension type pieces. The different trends seen in Fig.4 are not therefore due to the further problem of change of constraint between bending and tension or deep and shallow notches. Those further important problems are not discussed here. The materials cited include high strength steels, low alloy structural steels, general purpose C-Mn steels and a titanium alloy for a range of sizes from 10mm to 250mm ruling dimension, some with side grooves, some without. The

† Mechanical Engineering Department,
Imperial College of Science, Technology and Medicine, London.

cases shown in Fig.4 are all for one material, A533B, all taken from the literature whereas the cases cited but not illustrated cover all the patterns but in a variety of materials. None of the trends seem peculiar to any of these geometric or material variables in particular but rather, each contributes to the interplay of geometric and strength/toughness characteristics.It is argued that a general pattern is discernible in the several behavioural trends shown in Figs. 4 and 5 if the trends are related to the ratio between the toughness, expressed as a plastic zone size, and the ligament size, b. The zone size in question is the maximum possible that a sharp crack in a given material can sustain, denoted r_{mm}. Where the thickness is constant, the ratio between either B or b and the maximum plastic zone size for that thickness of the material, r_{mB}, also becomes relevant. The implication of a thickness effect on the maximum zone size for a given material relates of course to the degree of through thickness constraint developed, conventionally expressed as a tendency towards plane stress for thin cases and plane strain for thick.

Some of the marked similarities or differences of trends between data are highlighted in Table 1. Estimates of the plastic zone in contained plane strain yield were given by RDS in [23] as $c = 0.2\ EJ/\sigma_Y^2$ but the value appropriate to general plasticity is not clear when the conventional J value, as used in the R-curve analysis, continues to rise with growth.

TABLE 1 - Patterns of experimental behaviour and associated sizes.
Effect on J-R-curve as the stated range of size increases.

Material	A533B	C-Mn steel	HY130	Tit 6%Al
Source	[31][41][33]	[44][46]	[32][20][34][42]*	[19]
Side grooved	no 20% no	no no	no 20% no no	no
Width(mm)	higher[33]	slightly higher[44]	lower[32]	lower[19]
B, range of b	53, 39 to 75	13, 17 to 65	50, 6 to 33	35, 8 to 16
		higher[46]	none[20][34]	
		10, 5 to12	20, 9 to 43[20]	
			20,10 to 23[34]	
			23,10 to 48[42]*	
b/W ratio$	higher[41]	---	higher[32]	higher[19]
B, range of b	25,10 to 25	---	25,10 to 25	17, 9 to 22
Thickness(mm)	---	lower[44]	lower,then none[32]	none
range of B, b	---	12 to 50, 65	12 to 50, 25	4 to 35,16
Size(mm)	none[31]	none[46]	none,then lower[32]	lower[19]
range of B	10 to100	10, 24	25 to 50	10 to 40
range of b	5 to 50	5,12	12 to 25	5 to 20
		none,then lower[44]		
		37 to 50		
		50 to 65		

$ a/W all in the range $0.35 \le a/W \le 0.8$, but note here expressed using b/W. (N.B data of [41] showed only scatter until re-analysed in [36]).

* No R-curves are shown in [42], but data for plane sided pieces implies 'wider-higher'.

As a qualitative guide at this stage of the argument a value of $r_{mm}= 25J/\sigma_Y$ has been estimated for a value of J after an amount of growth $\Delta a = r_{pe,i} = EJ_i/6\pi\sigma_Y^2$ i.e. growth equal to the Irwin plane strain zone size at initiation. J values are taken from experimental data or by writing $J_{rp} = J_i + (dJ/da)_i\Delta a$. The data used and the values found, and the size for valid lefm plane strain conditions, here based on $2.5EJ_i/\sigma_Y 2$, are given in Table 2. The values for r_{mm} should be compared to the experimental sizes, thickness or ligament in Table 1, at which the size dependent changes in R-curve behaviour have been noted. It must be clear that the calculations made are quite speculative and that some of the values used could be altered by 50% or more from other data in the literature.

TABLE 2 - Data for and estimates of r_{mm} and other size factors.

Material	A533B;	C-Mn steels;	HY130;	Tit 6%Al
Source	[31][41][33]	[44] ; [46]	[32][20][34]	[19]
σ_Y MN/m^2	450	283 ; 285	890	728
J_i MN/m	0.15	0.06 ; 0.12	0.15	0.17
$r_{pe,i}$ (mm)	8	7 ; 14	2	2
c (mm)	32	28 ; 56	8	8
dJ/da (per mm)	0.40	0.08 ; 0.04-0.06	0.10-0.30	0.01to 0.04
J_{rp}	4.70	0.62 ; 0.68-0.96	0.45-0.70	0.19 to 0.25
$r_{mm} = 25J_{rp}/\sigma_Y$	260	55 ; 60-85	12-20	6 to 8
2.5 $(K_i/\sigma_Y)^2$ (mm)	400	370 ; 750	150	100

If the estimates in Table 2 were precise and the present arguments correct, i.e the estimated values of r_{mm} and of the experimental sizes were in complete accord, then the following patterns would emerge.

Geometrically similar pieces

In [31], a common curve was found with repect to absolute size for non-side grooved pieces of A533B, Fig.4a. All pieces, were much smaller than r_{mm} (= 260mm, Table 2). For C-Mn steel, Druce, [44] where only the largest size of piece is comparable to r_{mm} (55mm),the behaviour of the three smallest pieces is size independent, similar to [31], with the largest size giving a lower curve. This change in behaviour with size is also seen for HY130 in [32], Fig.5a, where for geometrically scaled sizes, the smaller pieces, taken to be smaller than r_{mm} (12-20mm), give results independent of size whereas the largest size, B = 50mm, b = 25mm, which is greater than r_{mm}, gives a lower curve. In [19] where even the smallest piece of titanium alloy, 10mm by 10mm, was no more than comparable to r_{mm}(6-8mm) the R-curves were 'wider-lower' over a 9-fold range of sizes, Fig.5b.

It thus appears that geometrically similar pieces will give the same J-R-curves, or a 'no-effect' pattern, provided the ruling size is smaller than the maximum plastic zone size possible for that material so that with increase in dimensions, all sizes scale, *within the plastic zone size* . In that circumstance, the material is dominated by the

general plasticity almost as if there were no crack, although it is not suggested that tearing does not occur.

Three effects of width

For the 'wider-lower' trend, such as Fig.4b, if the width were increased still further, a yet lower curve would be anticipated until, when the net stress on the ligament was sufficiently below yield, an lefm analysis could be used. For data such as Fig.4c where the curves follow a 'wider-higher' pattern, a width sufficient to allow an lefm analysis would presumably give a yet higher curve. Data for plain sided HY130 in [34] and for side grooved A533B, Fig 4d, show no effect of width, at least over the sizes reported.

For the series in [32] from which emerged the 'wider-lower' behaviour that scaled to an abscissa of $\Delta a/b_o$, the thickness of 50mm >> r_{mm} (=12-20 mm Table 2). For the titanium of [37] all the pieces in the 'size' and 'width' series were above r_{mm} (6-8mm). No two of the curves in those series were the same, a clear trend of 'larger or wider gives lower' being found when J_m was plotted against Δa as in [19]. If the lefm regime were reached for yet wider ligaments then control would change from $\Delta a/b$ to $\Delta a/c$ (where $c = r_{mB}$). Such a quasi-lefm R-curve could then be plotted on an abscissa of Δa since c is a constant for the thickness in question. The behaviour would be of a partly plane strain type giving predominantly flat fracture, regime ii of Fig.1. That R-curve could then be considered to be more or less lower bound for the thickness in question. The qualification 'more or less' recognises that there is an arbitrary small amount of plasticity included in the lefm analysis. Further discussion of how the change of abscissa might be made is given by Turner, [45].

As lefm is approached, the 'wider-higher' R-curve would surely be an upper bound for that thickness, tending to a shear-lip dominated fracture in essentially plane stress. In the 'wider-higher' series in [33] the thickness of A533B at 53mm was clearly much less than r_{mm}. This was also the case for the C-Mn steels in [44] and for [46], with thicknesses of 13 and 10mm respectively, compared to r_{mm} estimated as either 55 or 60mm (Table 2).

The'wider-no-trend' case of [34] seems balanced between the 'wider-higher' and 'wider- higher' behaviours. The 'wider-no-trend' case of Fig 4d seems to be an effect of small thickness and is discussed below with other thickness effects.

An effect of thickness and of side grooves

R-curves for HY130 constructed from the data of [42] show a 'wider-higher' trend for 23mm thick material contrary to the 'wider-lower' behaviour of [32] at 50mm thick. A change in behaviour for the geometrically similar pieces between 25mm and 50mm was noted, Fig.5a. In [34] 'wider-no-trend' data were reported at 20mm thick. Taken together, these data suggest that 20-25mm is a thickness close to point ii, Fig.1, above which HY130 is 'thick' but below which it is not.

However, in [18] the HY130 is also 20mm thick and thus comparable to r_{mm}, but the pieces are side grooved implying an effective thickness of much more than 20mm or zone size much smaller than r_{mm}. For the side grooved case a highly constrained zone size might be relevant, possibly that for c, Table 2, estimated as 8mm for HY130. These data, with B and b both greater than that value might well be near a minimum toughness comparable to the lefm plane strain regime, i, of Fig.1.

For the cases of side grooved A533B [20] a lack of effect of width is found in pieces that are only 12mm thick, Fig 4d, contrary to 'wider-higher' behaviour at 25mm thick and 'wider-lower' at 50mm thick. These latter two values embrace the value of c (32mm). The thickness of 12.5mm (9.6mm net) is perhaps one twentieth or less of the estimated value of r_{mm} and a third of c, well down limb iv of Fig.1, despite the side grooving, so that the small absolute value of thickness seems to dominate.

Thus these three cases appear to follow the 'no-trend' pattern for different reasons, some of which will be referred to again later.

AN EXPLANATION and DEFINITION OF dU_{dis}/Bda AND A RELATED R-CURVE

The titanium data of [19] was re-analysed in [37] in terms of the rate of dissipation of energy, dU_{dis}/Bda, for the combined plastic deformation plus tearing process.That re-analysis also showed why a scaled abscissa unified the wider-lower type of data.This analysis is described below.

During stable tearing the increment of external work, denoted 'total', in that it embraces the whole input to the test piece is

$$dU_{tot} = Pdq \qquad (13)$$

where P is load and q is displacement. This increment is expended partly in plastic deformation, dw_{pl}, partly against fracture resistance, RBda, and partly as an elastic term, dw_{el}. Thus

$$dU_{tot} = dw_{pl} + RBda + dw_{el} \qquad (14)$$

where U is work, w is internal energy and R is fracture resistance (work per unit area). Suffix 'el' is for the linear elastic and 'pl' for plastic component of the internal energy. The plastic and fracture components are necessarily positive. The elastic term may be positive for an increase of stored strain energy or negative for a reduction of strain energy. No suffix is put on the RBda term but the first question posed in Part I of this paper was whether the fracture term, RBda, can in fact be separated from the plastic term, dw_{pl}. Two alternative models of the process of fracture are examined.

As a first model, to cause a complete separation of a particle of material, i.e. an increment of growth, Δa, all the work done from 'before' to 'after' is termed 'fracture work'. In that model the terms dw_{pl} + RBda must be added together. For a second model, dU_{dis} remains the same but the elastic component of Eqn.14 is identified as 'fracture toughness'. This implies that

$$dU_{tot} = dw_{pl} \text{ and } RBda = - dw_{el} \text{ (provided } dw_{el} \text{ is -ive)} \qquad (15a,b)$$

Here it is argued that the meaning of 'fracture' must be the final 'coming apart' in an increment of growth, because there is no other distinguishing point between the start of deformation, 'before', and the separated particle, 'after'. In this model, crack opening stretch, blunting and all adjacent plastic flow is 'plasticity'. Creating a new surface at the tip of the blunted crack is the final 'coming apart'. This is perhaps the realm of semantics, but the meaning of 'fracture' in the final sense being discussed in this model must be the actual 'going ping', unstable on the *micro* scale (albeit here by a ductile process), which implies an elastic driving force. Stable tearing is then seen as a summation of plastic damage ahead of the tip, extending as remote from the

crack as may be, interspersed by microscopic 'actual fracture' events to cause the actual increment of growth, Δa.

The simple argument of looking at the overall load displacement diagram from conventional tearing tests to show that the 'plastic work of fracture' is second order, has already been noted in connection with Fig.2. Two actual diagrams of quite different shapes are shown Figs.6a), b). That for Fig.6a is similar to Fig.2 and is an early multi-test-piece record, Garwood,[47], for small pieces of ductile steel, En32, as referred to in [46]. Fig.6b, Braga & Turner, [48], is for the same titanium alloy as [19] and [37]. A rather similar diagram for HY130 is shown in Joyce, [49]. It has been suggested, Atkins, [50], that where there is a quite sharp change from a positive to a negative slope of the load displacement diagram, as in Fig.6b, then the maximum load can be identified with initiation of fracture. Even so, the difference between the 'without tearing' and 'with tearing ' increments in work done is still only second order in relation to the total increment of work, Pdq. As said before, the plastic deformation up to the point in question has damaged the material and

either that must be included in the fracture event (the first model here)

or the fracture event is only the change of the elastic component of energy that supplies drive for the 'actual fracture' (the second model here).

In [42] the fracture term was neglected as small relative to the total term. In the rigid plastic model of [50], where there is no elastic term to give a micro-instability, the present writer interprets 'separation' as being caused by continued plastic deformation ahead of the advacing tip as further external work is done on the body.

Both models are preserved by re-writing Eqn.14, using Eqn.12, as

$$D = dU_{dis}/Bda = dU_{tot}/Bda - dw_{el}/Bda \qquad (16a)$$

On that definition, available dissipation rate, D, is 'the work rate other than the recoverable energy rate'. In Turner, [51], the elastic energy release rate for elastic plastic material is defined as I so that Eqn. 16a becomes

$$dU_{dis}/Bda = dU_{tot}/Bda + I \qquad (16b)$$

For stable growth, Eqns.14 and 16 also mean

$$dU_{dis} = D_{applied}Bda = D_{material}Bda = dw_{pl} + RBda \qquad (17)$$

on which definition material dissipation rate is the 'combined plastic and fracture absorption rates'. Clearly, the term denoted D for 'dissipation', implies a d/Bda rate and an equality of the 'available' and 'consumed' term for a stable state. The first model of tearing identifies tearing toughness with dU_{dis}/Bda from Eqn.17 whereas the second implies it is $-dw_{el}/Bda$ from Eqn.15 or I from Eqn.16. The two models are entirely compatible in the physical sense but to some the distinction may appear semantic. For the rigid plastic model, dw_{el} is zero and there is no actual area of separation. For the first model dU_{dis} is the toughness, albeit all 'plastic damage'. In the second model there is no 'toughness' in the sense of RBda.

In the lefm case case dU_{tot} might be written dU_{el}, since dw_{pl} is zero, and the only dissipation is R_GBda where R_G implies that lefm has been used to evaluate the effective surface energy. In that case Eqns 14 become

$$dU_{el} = dw_{el} + R_GBda \qquad (18)$$

In a mathematical though not a physical sense, there is no plastic dissipation in lefm. All dissipation is just 'effective surface energy'. In fact it is generally accepted that in the Irwin-Orowan sense most of the fracture absorption is micro-plasticity. In lefm plane stress, or in lefm used with a plastic zone correction factor at some significant fraction of a fully plastic load, the plasticity term is not negligible even in the mathematical sense, but even so is not separated from the elastic term.

In the first model above, the same view is carried over into epfm so that 'tearing resistance' is identified with dU_{dis}/Bda. If the plastic component is objected to then tearing toughness can be identified with $-dw_{el}/Bda$. As seen from Fig.3, even at initiation that term is not G_{Ic} once plasticity is appreciable. With plasticity, it is the *combined* 'plasticity plus fracture' term that equates to G_{Ic}. It is remarked with no further comment that I_i (or I_{Ic}) seems as plausible a candidate as J_i (or J_{Ic}) for initiation in plasticity. An extension of the separation of plastic and elastic terms into the post initiation regime is given in [48]; in brief, the pattern of Fig. 3 is continued with stable tearing. The dU_{dis} term remains the sum of the plasticity and fracture components so that at this point either that sum or its elastic component seem the only candidates for the meaning of 'toughness', in answer to the original question of 'can tearing toughness be separated out'. The foregoing discussion has centred on the distinction between the increment of dissipation, plasticity and fracture combined, or the elastic 'final fracture' component only, surely measured by an increment. But the former can either be measured either by the increment dU_{dis}/Bda or by the conventional term J_r, defined by Eqn.10. This distinction, between the incremental or accumulated term will now be examined.

Interpretation of tearing by dU_{dis}/Bda

The reason for supposing that the increment might be more relevant than the total lies in the incremental nature of plasticity theory. It is generally agreed that incremental and total theory are very similar prior to initiation since the ratios of principal stress change but little with degree of plasticity, at least for the high constraint cases. It is less certain how the stress patterns change after initiation and into large amounts of growth, and whether those changes are similar for different sizes and configurations even within the high constraint types of piece.

Detailed analysis in support of the dU_{dis}/Bda picture has so far been made only for the titanium data in [37] from [35], within which two sets were treated, one for pieces mainly 17.5mm thick (referred to as 'thin') and the other for pieces 35mm thick (referred to as 'thick'), both plain sided. Closely related terms were used [41] for side grooved A533B and [42] for plain and side grooved HY130. In [41] the energy terms for stable tearing were described and then separated into several terms including one called 'the plastic energy dissipation rate' which differed from the total by an elastic term that appears to be GBda, i.e.- $\partial w_{el}/B\partial a|_q$. The present writer believes that that plastic energy term of [41] is not identical to the term here called D but that the plastic dissipation term of [42] is. This latter term differs from the total work rate by dw_{el}/Bda, as in Eqn.16. That elastic term can be either negative or positive in value according to circumstances, whereas $\partial w_{el}/B\partial a|_q$ is essentially negative.In [35], the elastic component of dU_{dis} was neglected on the assumption that for tests at general yield it would be negligible. In fact the elastic component of energy rate in the dU_{dis}/Bda term was some 20% for the larger pieces. In a physical sense its inclusion

is seen as important since it is the only term, as argued above, that can cause the 'final fracture'. In a numerical sense its exclusion, [35], or different treatment, [41], is not crucial at limit load.

The fact that dU_{dis}/Bda seemed to scale, as distinct from a suggestion that it might simply be a more appropriate measure than the conventional rising J-R-curve, was first noted in [36] in relation the data for the tearing of side grooved A533B steel using compact tension loading, itself re-analysed in [41] using data from Vassilaros *et al*, [52]. Thus the scaling onto an abscissa of $(\Delta a/b_o)(S/b_o)$ of two sets of quite detailed data, one for A533B from [41] as seen in [36], and the other for titanium in [37], quite separate in material, configuration and laboratory, strongly suggested that the scaling was meaningful rather than fortuitous. Selected data for these two cases are shown Fig.7 using an abscissa of Δa and the same data in Fig.8, using a scaled abscissa of $(\Delta a/b_o)(S/b_o)$, where b_o is the original ligament size and S is the span in bending or the moment arm in compact tension.

If used as a type of tearing resistance curve in the fully plastic region, these measures either fall strongly with growth, [37]('thin'),[41],[42](side grooved), or but little [37] ('thick'), [34], or not at all, [42](plain sided), whereas the conventional J-R-curve rises strongly with growth. It is important to note that the single curve of dU_{dis}/Bda against a scaled abscissa of $(\Delta a/b_o)(S/b_o)$ has only been examined for J-R-curves with a 'wider-lower' trend. The relation between the falling dU_{dis} curves of Figs.7 & 8 (from 'wider-lower' cases in [37] and [41]&[52]) and a conventional rising R-curve is discussed next. A further interpretation of the dU_{dis} values in [34] and [42] that come from 'wider- higher' or 'wider-no-trend' cases and are nearly independent of growth is discussed later.

A Related Dissipation R-curve

If the behaviour outlined above is accepted then an R-curve, no doubt better now called a Dissipation or D-R-curve rather than a J-R-curve, can be defined by

$$D_{mat} = J_i + SdR_{dis} \qquad (19), \text{ where}$$

$$dR_{dis} = hdU_{dis}/Bb_c \qquad (20)$$

Examples of these D_{mat} or R_{dis} curves and comparison with J_m, are shown Fig.9a, from [37], for a series of various widths giving the 'wider-lower' pattern.

By re-arranging Eqn.20 as

$$dR_{dis} = h(dU_{dis}/Bda)(dx)/[(S/b_o)- x] \qquad (21)$$

where x is the abscissa $(\Delta a/b_o)(S/b_o)$, it can be seen that dR_{dis} would be the same for an increment, dx, irrespective of the value of b_o, provided h and S/b_o were constant, i.e. R_{dis} would be independent of b_o on an abscissa of $\Delta a/b_o$. The cases from Fig.9a are shown, Fig. 9b. The data from [41] and certain cases from [37], including Fig.7a, where a/W was the geometic variable, although scaling for D as in Fig.8 do not give a single R_{dis} curve because S/b_o varies. It will be clear that the style of R_{dis} as normalised energy per unit ligament area is the same as for a conventional J-R-curve but its relation to the J-integral has vanished.

For the 'wider-higher' data it seems likely that the ordinate of a J-R or strictly a D-R-curve, would scale according to the maximum tearing dissipation rate possible for

the material; the abscissa would scale with the factor, material zone size, r_{mm}, or geometric size B or b, that controlled the dissipation rate for the material and geometry in question. For purposes of comparison only, when there is a factor on one or both axes common to two sizes then the normalisation can be omitted. That would certainly be so for the case of well contained yield, as in [23], and for the 'no-effect' case of geometric similarity of dimension and zone size. Few R-curve data with details sufficient to explore these suggestions are available in the published literature though may well exist in original unpublished records.

A MORE GENERAL PICTURE OF TOUGHNESS

Discussion of Scaling Factors

The factors that control the scaling of dU_{dis}/Bda would vary from case to case from r_{mm} for pieces large in relation to zone size to B or b for pieces not large in relation to zone size. In the latter case a term r_{mB} can also be envisaged, itself governed by the interplay of r_{mm} and B. This would be consistent on with the RDS picture, [23], for contained yield but with their normalised abscissa embracing several possibilities, as already discussed, and their normalised ordinate, J/J_{Ic}, now translated to D/D_{mB}, where D_{mB} is the dissipation rate corresponding to the formation of r_{mB} (including the r_{mm} case where appropriate) in the fully plastic condition.

Firstly it is asked why the group $(\Delta a/b_o)(S/b_o)$ is the appropriate scale factor for the abscissa of the 'wider-lower' data. The increment of work in three point bending is

$$dU = (dU/da)da = Pdq = L\sigma_Y Bb^2 dq/S \qquad (22)$$

so that

$$dU/Bda = (L\sigma_Y dq)(b^2/Sda) \qquad (23)$$

where L is regarded as a loading factor that increases from zero to some fully plastic value. Clearly, with tearing, da will be some function of $L\sigma_Y dq$ and each increment dU/Bda is a multiple of (b^2/Sda) so that, inverting the dimensionless group to the form commonly used, then for successive increments, dU/Bda can be represented as $f(\Delta a/b)(S/b)$. The grouping of geometric terms will not change with the stress strain law so that elastic, plastic, total or disssipated components of energy, including dU_{dis}/Bda from Eqn.16, will be a function of the same non-dimensional group.

The question remains why the experimental data of Fig.8 appear to scale with b_o rather than with the current value b_c, which of course governs the fully plastic moment. It is supposed from Eqn.20 that this dependence must be governed by the little known functional relationship of da on dq. In so far as the titanium data and the HY130 data of [34] relate to the load displacement curve of the 'pagoda roof' type, Fig.6b, it seems that initiation in these pieces occurs little if any beyond first reaching the fully plastic state so that the dU_{dis}/Bda value will reflect the initial size dependent degree of hardening up to initiation. That the HY130 material of [34] was relatively little hardened at initiation or at maximum load (which points were quite close together) was seen, Dagbasi & Turner, [53], where the high L factors found after initiation, surely reflect that appreciable hardening was still occuring late in the tests, post maximum load, contrary to the near exhaustion of hardening prior to the

maximum load in the conventional un-notched tensile test. Computational models of these data also supports this view, Xia & Turner, [54]. In short, the energy dissipation rate that is being measured relates more to the state of the material at initiation, a state for which the amount of deformation is *initial-size* dependent, than to the state a test piece of current ligament size would have reached had it been taken to its maximum load at that smaller size.

The above remarks apply more strongly to the falling regime of the dU_{dis} curves where growth is in the region only just ahead of the initial crack tip, and initiation seems to occur just before or at maximum load. If a true plateau regime for D were approached, at larger amounts of growth in Fig.8 or for any growth in Fig.11b then the choice of b_o or b_c and indeed the whole non-dimensional group for the abscissa, becomes irrelevant. The question of whether a set of 'wider-higher' could be scaled to give a single curve, as for the 'wider-lower' cases is not clear. In [30] an empirical relation was noted that for one set of J-R-curves from [20] scaled on an abscissa of $(\Delta a/S)b_o^2$. That treatment is also reasonable for the 'wider-higher' A533B data in [33] and En32 data in [28] and [46]. The abscissa was seen as implying a $(size)^2$ effect as the plastic zone became larger with size of piece. A more rational argument for such cases might be that the abscissa remains the same, $(\Delta a/b_o)(S/b_o)$, for all cases, but the work is a function of the *volume* of the plastic zone so that dU_{dis}/Bda would itself scale with zone size. This implies that a corresponding R-curve would scale on both axes by some size factor. No suitable experimental evidence is known. Some J-R curve data for En32 from [28], albeit in terms of J_r rather than R_{dis}, is shown Fig.10a and scaled satisfactorily on both axes, Fig.10b. In a fuller study the question using a common J_i value and scaling only the increments above initiation must surely arise but to within the accuracy of Fig.10 that point is not persued here.

Two relevant sets of HY130 data, [34] at 20mm thick and [42] at 23mm thick can also be examined. Curves of U_{dis}/B and dU_{dis}/Bda are shown Fig.11, corresponding to J-R-curves of a 'wider-no-trend' pattern. The dU_{dis}/Bda trend in [34] reduces quite strongly for a very small amount of growth followed by plateaux with values that are higher for wider ligaments. In [42] R-curves are not shown, although the writer deduces they must have been of the 'wider- higher' type, with the U_{pl}/B curves (also not shown) described as some being linear and some not quite linear, much as shown for Fig.11a. But dU_{pl}/Bda values are shown with no reducing regime, but as invariant with Δa and strongly ligament size dependent, Fig.11b.

The writer suspects that at the inclusion or exclusion of a reducing trend at small Δa, reflects the treatment of the data to obtain dU_{dis}, point by point in [34] to give Fig.11a but by regression analysis in [42] to give Fig.11b. Only re-examination of the raw data or preferably a much wider data base can tell whether these differences are real or whether, as the writer believes, that to within the accuracy of the data, the behavioural pattern is not contradictory, there possibly being a small region with a decrease in dU_{dis}/Bda followed by plateaux that are ligament size dependent. Some differences in the trends might be accounted for by the differences due to variability between plate samples, possibly the orientation of the test samples and the lack of R-curves prepared to a common formula.

It was remarked in connection with Table 2 that in order to evaluate the plastic zone size r_{mm} from an ever rising J-R-curve, the choice of value of J was uncertain. In the light of these arguments it is now suggested that after initiation, D rather than J

(or R) is the factor that characterises the size of the active plastic zone. That zone would tend to a steady state size as, or if, the value for D reaches a plateau for large amounts of growth, Figs.8 or 11.

Areal and Volumetric Dissipation Rates?

The plain sided data of [42], Fig.11b, are independent of Δa on the abscissa although the side-grooved data reduces and might scale if other sizes were avaliable for comparison. For the plain sided pieces the ordinate also show a strong effect of ligament width so that if R-curves are constructed a 'wider-higher' pattern emerges. It is now suggested that the dissipation rate for the plateaux in Figs.11a and b can be further analysed by writing

$$DBda = dU_{dis} = \gamma B da + \rho c c da \qquad (24)$$

where γ is an energy per unit area for flat fracture, ρ is an energy per unit volume for slant fracture and c is the related size dimension in the thickness and span directions. This treatment extends the picture of [36] where only the ρ term was used and also extends the suggestions in [28] and [18] that flat and slant components of the R-curve could be identified, but to the D (rather than R) curves. Clearly the analysis could not be applied if there were no scaling of the D curves for some geometrically similar cases, but no data are known. For the curves ii) and iii) of Fig.10 with c = 0.45b, the tensile part of the ligament, the analysis gives

$$\gamma = 0.60\ MJ/m^2,\ \rho = 450 MJ/m^3 \qquad (25)$$

It must be noted that the absolute value of ρ would be altered if some other fraction of ligament were used for c. The value of γ is the same as that for large growth in the side grooved piece, curve iv) of Fig.10 but appreciably more than that usually taken for J_{Ic} for HY 130 (a value is not given in [42] but e.g 0.15MN/m. Table 2). When both the thickness and ligament (or perhaps more strictly, half the thickness and 0.45b) are close to r_{mm} then a maximum dissipation rate might be expected and in [42] the B = 23mm, b = 46mm case, Fig.10 curve i), is close to that condition. Applying these values to curve i) gives D = 9MN/m compared to the experimental value of 10MN/m.

Finally, it is remarked that a somewhat similar analysis was proposed by Cotterell & Mai, [55] where the work done for *complete* separation were of the form U/Bb = a + bb. The partly areal partly volumetric dependency of toughness, here analysed through Eqn. 24, was noted experimentally, albeit for blunt notch tests, some 60 years ago, by Docherty [56]. It seems a happy coincidence that the symbol D may help commemorate that insight.

A general picture of effects of size on tearing toughness

In the lefm picture of Fig.1, regime i relates to configurations with sufficient size for B, a and b all to satisfy the plane strain lefm size requirement, Eqn.3, so that when B is large, b ≥ B. For small thicknesses, in the lefm plane stress regime (where $r_{mm} > r_{pl} \approx B$), then b >> B to avoid yielding of the ligament. A tentative form of a more general diagram is suggested Fig.12, whereby in a region iv of small pieces, such that $r_{mm} > B$ and b (or perhaps B/2 and 0.45b) the characteristic features are that at constant thickness the epfm R-curves are of the 'wider-higher' pattern whereas for the 'no-effect' geometrically similar pieces with comparable B and b values, the R-curves

are the same, regime iii. The implication is that dissipation (expressed per unit area) is dominated by plasticity throughout a volume rather than by crack tip behaviour. There is next a regime ii where the R-curve is restricted by r_{mm} < B or b so that the 'wider-lower' pattern is followed, finally reaching lefm plane strain in regime i where $r_{pl,e}$ < (B or b)/50. The shape of regime ii may also depend on the ratio B/b and it is not clear whether the 'wider-no-trend' cases, presumably in between regimes ii and iii, are restricted to certain B/b or b/r_{mB} values. Because of the rather small range of sizes and proportions embraced by most laboratory test data, it is not surprising that no evidence is known to the writer where a wide range of these effects can be seen as a convincing pattern within one set of results.

Nor does this picture in terms of the conventional measure of toughness reveal that, despite the contrary conclusions made after Eqn.18, splitting dU_{dis}/Bda into areal and volumetric terms now appears to offer an answer to the separation of energies provided the analysis is by D not J.

DISCUSSION OF FINAL INSTABILITY

Ductile instability was seen to occur, Turner [51] when the elastic energy release rate available, I, exceeded the energy dissipation rate. The term I, for the test piece, with or without suffix s for the whole system, was evaluated using an overall elastic-plastic value η_o as

$$I_s = G + G^* = G[(\eta_{os}/\eta_{el}) - 1] \qquad (26)$$

The terms η_{os} and thus G* are configuration dependent, including the system stiffness when that is represented as an effective length or span of the test piece, Etemad & Turner, [57]. The immediate point is that the dissipation rate has hitherto been obtained by unscrambling the value of the term required from a particular J-R-curve, according to the definition of J used after initiation, Eqn 12. The statements of stable ductile tearing and tearing instability, when there is no work input to the whole system, are now unified as

$$D_{app} = dU_{tot}/Bda + I = dU_{tot,s}/Bda + I_s = D_{mat}\ ; \quad I_s \geq D_{mat} \qquad (27)$$

(stable) (unstable)

where $dU_{tot,s}/Bda$ and I_s include the work increment to and energy release from the whole system. The further point on whether this first or second derivative of energy controls the instability is only entered into here briefly; both of course must be satisfied.

A convex (or 'round-house') diagram as in Fig.6a, is quite similar to the normal unnotched tensile necking behaviour whereas the 'pagoda roof' type of Fig.6b, concave after maximum load, is quite different. The writer suspects that the 'round-house' type of tearing diagra allows much more hardening before maximum load than does the 'pagoda roof' type. This difference in the remaining hardening capacity may well affect both the form of the diagrams and the nature of any instability. The I analysis has been applied only to the Fig.6b type diagram which was found [57] for HY130 and [35] for titanium. It seems that if instability occurs at all, it will be very near the maximum load where almost any machine compliance will allow satisfaction of the second derivative. Control is then exercised by the first derivative of energy, Eqn.26, such that the 'plastic damage' done by the compliance dependent term G* is sufficient to allow G to trigger the actual instability. Thereafter, the concave shape of

the curve makes unstable behaviour less likely or arrest of an unstable crack sometimes possible. For a diagram of the type of Fig.6a, the second derivative is the determining factor as for the conventional necking instability, with arrest for a given compliance possible only if some concavity occurs, as indeed seems to be so towards the very end of Fig.6a. Schematic machine stiffness lines are shown on Fig.6 to illustrate these points. The instability arguments will be persued in more detail elsewhere.

CONCLUSIONS

All remarks here refer to the deep notch bend geometries. Although the concepts could be adapted to tensile loadings that has not been attempted so that no conclusion is offered on whether a relation could be established between the bend and tension types of dissipation.

A rather general pattern of behaviour has been outlined in terms of D (= dU_{dis}/Bda) that embraces many of the observed trends of experimental J-R-curve data, including the 'wider-lower', 'wider-no-trend', 'wider- higher' and 'no-effect-of-size' patterns.

The governing factor is seen as the ratio between size and material toughness expressed as a maximum plastic zone for a given material, r_{mm}. For the 'wider-lower' behaviour scaling of D versus $(\Delta a/b_o)(S/b_o)$ is appropriate. For the 'no-effect' cases of total geometric similarity no scaling is needed. For the 'wider- higher' cases scaling of both axes is suggested but more data are needed.

Increasing toughness, as measured by the conventional J-R-curve, reflects an increase in the cumulative energy dissipated. Whilst the size of plastic zone is increasing then the rate of energy dissipation is also increasing so that normalised cumulative work, J, or energy rate, d/Bda, meanings of toughness can be related. When the size of active plastic zone is decreasing, the normalised cumulative work increases but the d/Bda rate, decreases. The measure, D, seen as the 'current' toughness can be related to the 'historic' toughness for cases where the loading path history is similar through the particular cumulative measure, R_{dis}, which is equivalent in style to the conventional J-R-curve. A method of translating the 'wider-lower' R-curve cases to the lefm regime is foreseen.

D reduces to G for the lefm case of tearing at constant load; it reduces to the RDS case of the increment of external work in the rigid-plastic case; it describes stable growth in a manner that is consistent with the I energy rate model of ductile tearing instability.

When the dissipation rate, D, is a function of size, it can be split into areal and volumetric components, offering a more quantitative treatment of size effects in ductile tearing.

SYMBOLS USED: PART II

c = the dimension that controls the size of plastic zone, sometimes r_{mm}, B or b

I = the elastic energy release rate in an elastic-plastic system

γ = flat fracture energy per unit area
ρ = slant fracture energy per unit volume

REFERENCES: PART II

44) Druce, S.G., ICF-5(2), Ed Francois, 1980 pp 843-54.

45) Turner,C.E., A relationship between R-curves in uncontained and contained yield. Presented, 22nd Nat Symp Fract, Atlanta, 1990.

46) Garwood,S.J. & Turner,C.E., Fracture 1977 (Univ Waterloo, 1977) Ed.Taplin, D.R. pp.279-284.

47) Garwood,S.J., Ph.D. Thesis, Univ London, 1976.

48) Braga, L. & Turner,C.E., Energy changes during ductile tearing. Idem 45.

49) Joyce,J.A., ASTM STP 803, Am Soc Test Mats, 1983, pp. II..439-II..463.

50) Atkins,A.G., Energy considerations indeformation transitions. Future Trends in Applied Mechanics, Univ Athens, 1989, pp.325-37.

51) Turner, C.E, ASTM STP 677, Am Soc Test Mats 1979, pp.624-628.

52) Vassilaros,M.G., Joyce,J.A. & Gudas,J.P., STP 700, Am Soc Test Mat, 1980, pp251-270.

53) Dagbasi,M. & Turner,C.E., Int J Fract, 42, 1990, pp.R15-R18.

54) Xia,L. & Turner,C.E., An improved model for an advancing crack. 3rd Int Conf Numerical Methods, Freiburg, April 1990. To be published.

55) Cotterell,B. & Mai,Y.W., Int J Fract, 20,1982, pp.243-50

56) Docherty,J.G., Engng, June 1932, p.135 & p.645, and Feb 1935, p.139 & p.211.

57) Etemad,M.R. & Turner,C.E., STP 905, Am Soc Test Mat,1986, pp.485-502.

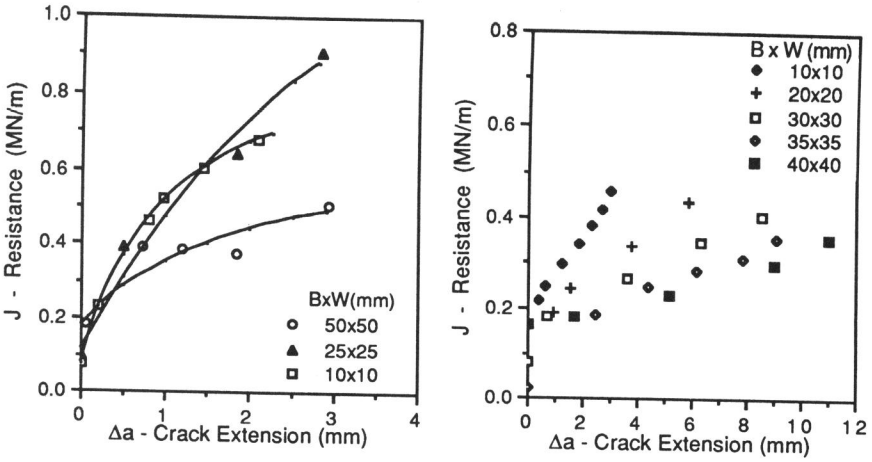

a) size independent up to a certain size then 'bigger-lower' for HY130, [32].

b) 'bigger-lower' over a nine-fold range of sizes for a titanium alloy, [19].

Fig.5. Some other trends with geometrically similar pieces.

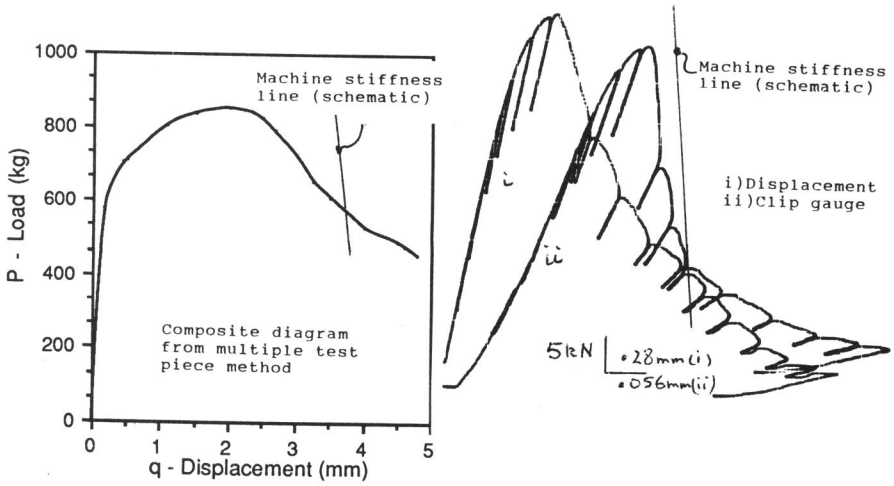

a) for En32, [47].

b) for titanium, [48].

Fig.6. Load-displacement diagrams for stable tearing.

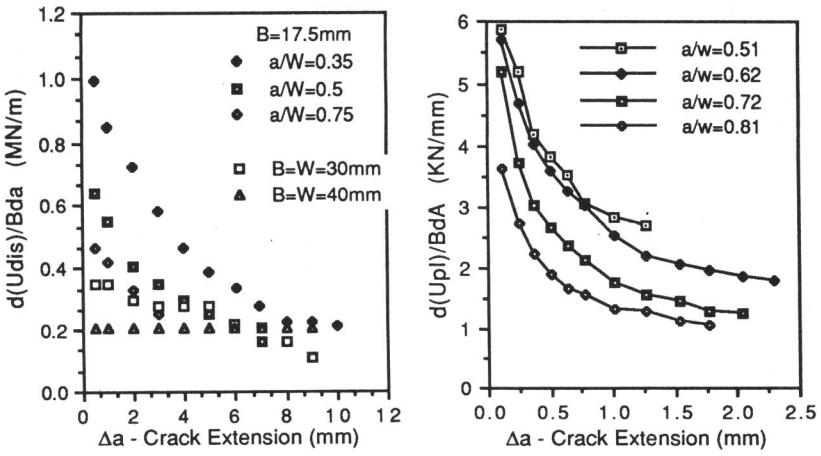

a) titanium alloy, [37]. b) A533B, [41].

Fig.7. Dissipation rate, dU_{dis}/Bda as a function of crack growth, Δa.

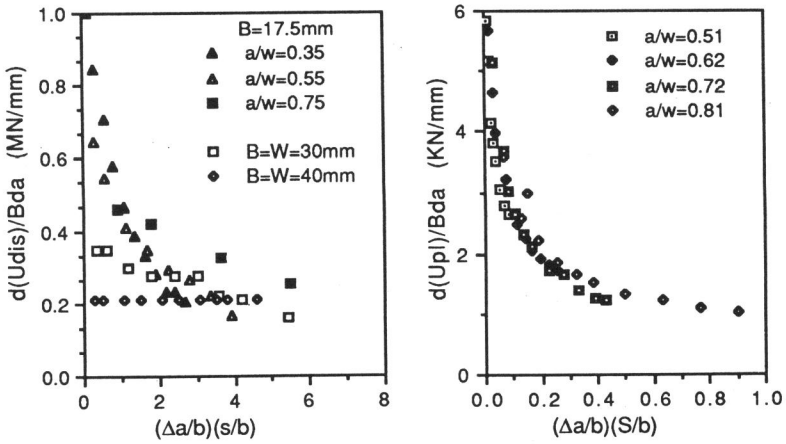

a) titanium alloy, [37]. b) A533B, [41].

Fig.8. The data of Fig.7 scaled to an abscissa of $(\Delta a/b_o)(S/b_o)$.

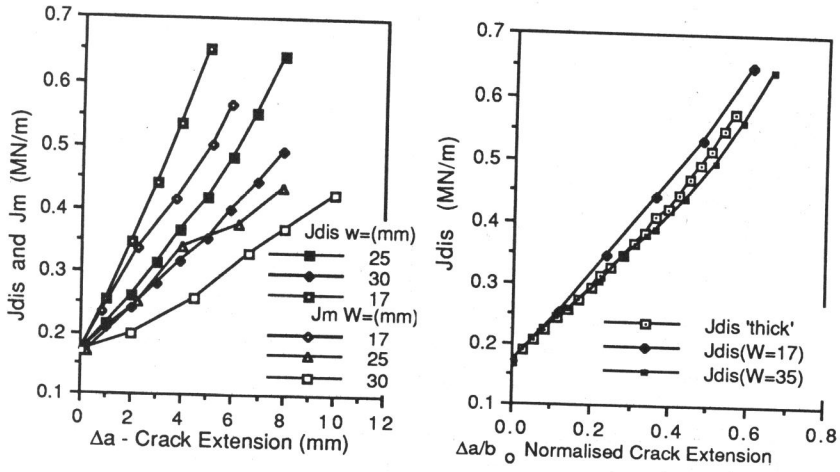

a) as a function of Δa.

b) scaled to an abscissa of $\Delta a/b_o$.

Fig.9 R_{dis} for various widths of three point bend pieces and comparison with J_m for a titanium alloy from [37].

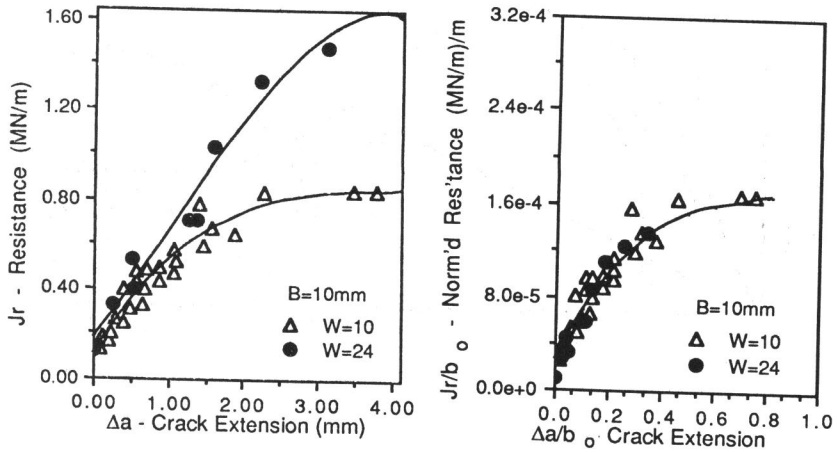

a) J as a function of Δa, [28].

b) J/b_o as a function of $\Delta a/b_o$.

Fig.10. 'Wider-higher' J-R-curves for En32;

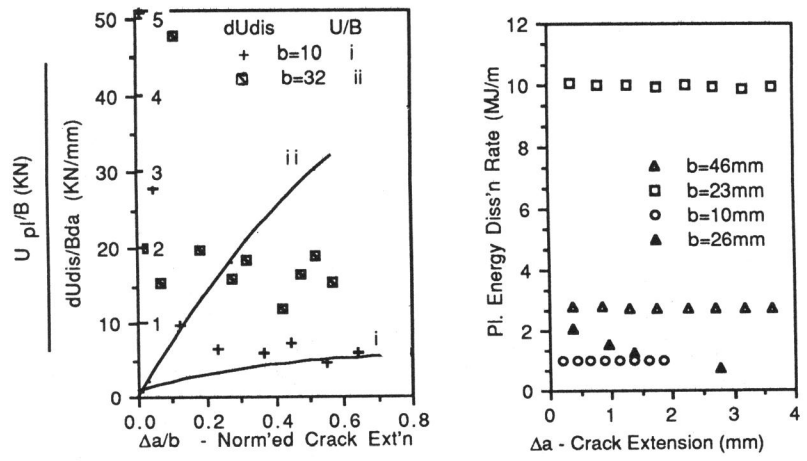

a) from [34], also showing cumulative U_{dis}/B. b) from [42]; i) b_o =46mm, ii) b_o=23mm, iii) b_o= 10mm plain sided, iv) b_o=26mm side grooved.

Fig.11. Dissipation rate curves for 20mm (approx) thick HY 130;

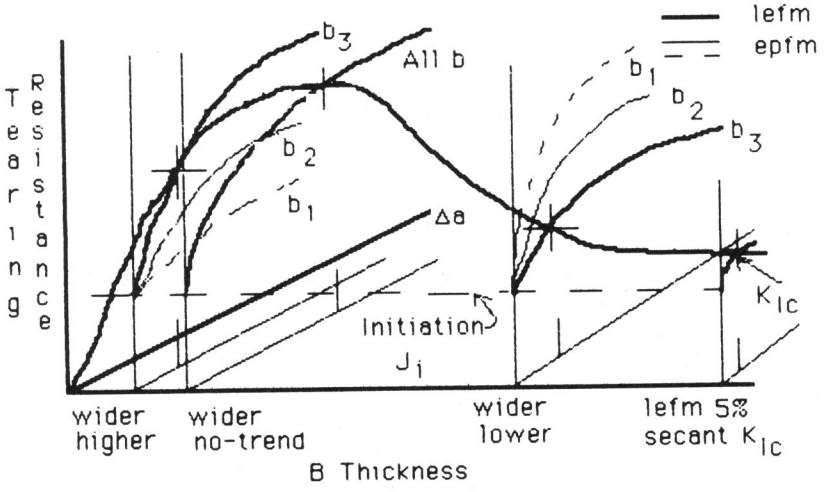

Fig.12. Schematic generalisation of toughness, R, as a function of thickness, crack growth and ligament size.